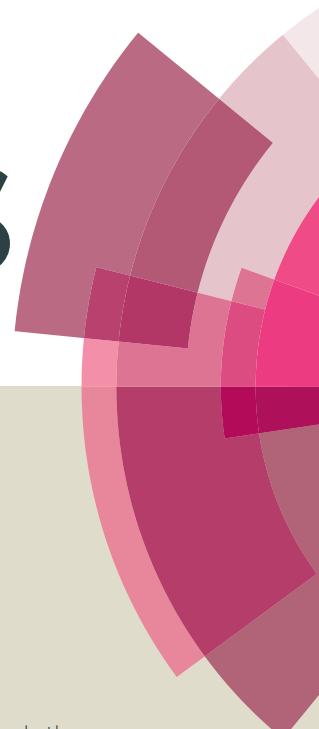


RSC Advances



This article can be cited before page numbers have been issued, to do this please use: Y. Dai, X. Liu, P. Wang, J. Fu, K. Yao and K. Xu, *RSC Adv.*, 2016, DOI: 10.1039/C6RA23296E.



This is an *Accepted Manuscript*, which has been through the Royal Society of Chemistry peer review process and has been accepted for publication.

Accepted Manuscripts are published online shortly after acceptance, before technical editing, formatting and proof reading. Using this free service, authors can make their results available to the community, in citable form, before we publish the edited article. This *Accepted Manuscript* will be replaced by the edited, formatted and paginated article as soon as this is available.

You can find more information about *Accepted Manuscripts* in the [Information for Authors](#).

Please note that technical editing may introduce minor changes to the text and/or graphics, which may alter content. The journal's standard [Terms & Conditions](#) and the [Ethical guidelines](#) still apply. In no event shall the Royal Society of Chemistry be held responsible for any errors or omissions in this *Accepted Manuscript* or any consequences arising from the use of any information it contains.

A new fluorescent probe based on quinoline for detection of Al³⁺ and Fe³⁺ with “off-on-off” response in aqueous solution

Yanpeng Dai^a, Xiaoyan Liu^a, Peng Wang^a, Jiaxin Fu^a, Kun Yao^a, Kuoxi Xu^{a, b*}

Abstract: A new quinoline-based fluorescent probe **1** has been designed and synthesized. Fluorescence emission spectra of the probe showed red-shift and obvious enhancement of fluorescent intensity upon the addition of Al³⁺ (turn-on). **1**-Al³⁺ showed high selectivity for Fe³⁺ over other metal ions, and eliminated the interference of Al³⁺ during Fe³⁺ detection (turn-off). It showed highly selective relay recognition of Al³⁺ and Fe³⁺ via a fluorescence “off-on-off” mechanism. Fluorescence spectra indicated that the response of **1**-Al³⁺ to Fe³⁺ was caused by central metal displacement. The detection limits for the analysis of Al³⁺ and **1**-Al³⁺-Fe³⁺ ions were calculated to be 2.20×10⁻⁶ M and 1.96×10⁻⁵ M, respectively. The living Hela cells imaging studies revealed that the probe was cell-permeable and it could be used to detect intracellular Al³⁺ and Fe³⁺ ion.

1. Introduction

Metal ions play an important role in living organisms since they are involved in many biological processes such as osmotic regulation, catalysis, metabolism, biomineralization and signaling¹⁻⁶. However, abnormal concentration levels of metal ions might cause detrimental effects, for example, Al³⁺ is an essential metal ion in human health but is also harmful to biological systems in excessive amounts⁷. Al³⁺ can cause damage to the central nervous system and the immune system of humans⁸, and affects the absorption and use of other trace elements⁹. Excess of Al³⁺ can cause microcytic hypochromic anemia, Al-related bone disease, encephalopathy and neuronal disorder that will lead to dementia, myopathy and Alzheimer's disease¹⁰⁻¹³; Fe³⁺ is an essential transition metal ion in human body, which plays a crucial role in the growth and development of human body involved in oxygen uptake, oxygen metabolism, and electron transfer process¹⁴⁻¹⁶; It also be involved in the underlying mechanisms of many neurodegenerative diseases such as Alzheimer's disease and Parkinson's disease^{17, 18}; Lack or accumulation of Fe³⁺ in the body results in a variety

^a Engineering Laboratory for Flame Retardant and Functional Materials of Henan Province, Henan University, Kaifeng, 475004

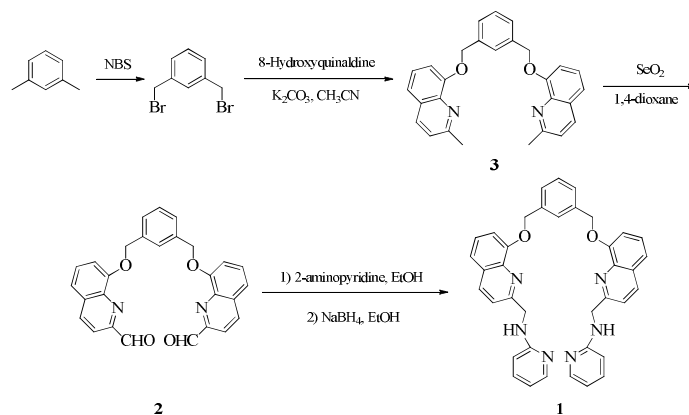
^b Institute of Environmental and Analytical Sciences, Henan University, Kaifeng, 475004

* Corresponding author, Tel./fax: +86 371 23881589; E-mail address: xukx@henu.edu.cn

of diseases and disorders¹⁹. However, both metal ions are extensively employed in industry, military affairs and agriculture, so it is urgent to develop highly sensitive probes for the effective detection of Al^{3+} and Fe^{3+} in biological and environmental systems, but only few Al^{3+} and Fe^{3+} ions probes were reported in the literature²⁰⁻²³. However, synthetic probes for selective detection of trivalent metal ions (Fe^{3+} , Al^{3+} and Cr^{3+}) without interfering from each other counter ions are rare. According to the widespread applications of Al^{3+} and Fe^{3+} ions in biology and environment, it deserves to proceed more researches²⁴⁻²⁶.

In general, as Al^{3+} is a hard-acid, it has been found that Al^{3+} prefers a coordination spherecontaining nitrogen and oxygen atom as hard-base donor sites. 8-Hydroxy quinoline is known to be good ligand for selective detection of alkali, alkaline earth and transition metal ions²⁷⁻³⁰. The derivative of 8-hydroxy quinoline contain nitrogen–oxygen-rich coordination sites which provide hard-base environment for the hard-acid Al^{3+} . Though many fluorescence probes are reported for the detection of Al^{3+} ³¹⁻³⁴, most of these probes use fluorescence ‘turn-off’ mechanism, few probes are found in the literature use ‘turn-on’ mechanism. So develop new fluorescent Al^{3+} and Fe^{3+} probes are still challenge.

Obviously, different recognition patterns lead to multiple fluorescence behaviors for detecting analytes, and thus rationally designing fluorescent molecular probes are indispensable for differential responses towards multiple metal ions. To address the above issues, we designed a novel probe **1** derived from 8-hydroxyquinaldine and m-xylene fragment (Scheme1) with multiple donor atoms for fluorescence detection of Al^{3+} and Fe^{3+} ions in aqueous solution. As we anticipated, probe **1** exhibited high selectivity for both metal ions, and its ‘turn-on’ behavior for Al^{3+} ions distinguished from the ‘turn off’ recognition behavior for Fe^{3+} ions maybe because they often cause the different spectral changes upon binding with their probe molecules. To the best of our knowledge, probe **1** represents the first example of simultaneous fluorescence detection and discrimination of Al^{3+} and Fe^{3+} ions in a aqueous solution at physiological pH.

Scheme 1. Synthesis of dipodal compound **1**.

2. Experimental Section

2.1 General methods:

All reactions were conducted in oven dried glassware. Solvents used for the experiments were distilled or dried as specified. The following chemicals were procured commercially and used without further purification, 2-aminopyridine, SeO₂, m-xylene, N-bromobutanamide, sodium borohydride and 8-hydroxyquinaldine. All other reagents and solvents employed for synthesis were commercially available and used as received without further purification. Column chromatography was done using 200-300 mesh silica gel and appropriate mixture of petroleum ether and ethyl acetate or chloroform and methanol system were used for elution.

2.2. Synthesis of probe **1**

The synthetic route of probe **1** is shown in Scheme 1.

2.2.1 Synthesis of compound **3**

A mixture of 8-hydroxyquinaldine (0.96 g, 6 mmol) and anhydrous potassium carbonate (1.25g, 9 mmol) in dry acetonitrile (10 mL). This mixture was stirred at 80 °C for 10 min. Then, a solution of 1,3-bis(bromomethyl)benzene (0.79 g, 3 mmol) in dry acetonitrile (10 mL) was added slowly to the mixture and the resulting solution was then stirred at 80 °C. The reaction mixture was stirred at this temperature until the reaction was complete as indicated by TLC (12 h). Potassium carbonate was filtered off and solvent was removed under reduced pressure. The remaining residue was extracted three times with chloroform. The combined organic layer was washed

with saturated brine and dried over anhydrous sodium sulphate. After the solvent was removed, the residue was purified by silica column (eluent ethyl acetate : ethylacetate = 8 : 1) to get a white solid in 80% yield. ^1H NMR (300 MHz, CDCl_3) δ (ppm) 7.94 (d, $J = 8.4$ Hz, 2H), 7.63 (s, 1H), 7.43 (d, $J = 7.5$ Hz, 2H), 7.34 (d, $J = 7.4$ Hz, 1H), 7.27 (d, $J = 7.8$ Hz, 4H), 7.20 (d, $J = 8.1$ Hz, 2H), 6.92 (d, $J = 7.5$ Hz, 2H), 5.42 (s, 4H), 2.76 (s, 6H).

2.2.2 Synthesis of compound 2

To a solution of **3** (1.26 g, 3 mmol) in 1,4-dioxane (25 mL), selenium dioxide (0.83 g, 7.5 mmol) was added and reaction mixture was stirred at 90 °C for 12 h. The dioxane was removed under vacuum and the residue obtained was treated with water (30 mL) and extracted three times with chloroform. The combined organic layer was washed with saturated brine and dried over anhydrous sodium sulphate. After the solvent was removed, the residue was purified by silica column (eluent ethyl acetate : ethylacetate = 6 : 1) to get a yellow solid in 86% yield. IR (KBr): 3402.12, 3051.32, 2822.28, 1712.57, 1611.55, 1504.02, 1428.81, 1324.02, 1238.07, 1104.23, 986.17, 834.40, 753.22, 696.45, 614.53, 470.53 cm^{-1} ; ^1H NMR (300 MHz, CDCl_3) δ (ppm) 10.26 (s, 2H), 8.27 (d, $J = 8.5$ Hz, 2H), 8.06 (d, $J = 8.5$ Hz, 2H), 7.74 (s, 1H), 7.55 – 7.50 (m, 3H), 7.46 (t, $J = 6.8$ Hz, 4H), 7.12 (d, $J = 7.4$ Hz, 2H), 5.50 (s, 4H). ^{13}C NMR (100 MHz, CDCl_3): 193.83, 171.17, 155.03, 151.54, 140.21, 137.29, 131.40, 129.60, 126.74, 125.61, 120.04, 177.88, 111.03, 70.94; **MS**: Calcd for: $[\text{M}+\text{Na}]^+$: 471.13 ; Found: 471.21.

2.2.3 Synthesis of compound 1

To a solution of **2** (0.45 g, 1 mmol) and 2-aminopyridine (0.24 g, 2.5 mmol) in ethanol absolute (20 mL) at 60 °C stirred for 12 h under nitrogen atmosphere. Then sodium borohydride (0.14 g, 3.8 mmol) was carefully added to the solution. The reaction mixture was stirred at this temperature for 12 h. Then, EtOH was removed under reduced pressure and the residue obtained was treated with water (30 mL) and extracted three times with chloroform. The combined organic layer was washed with saturated brine and dried over anhydrous sodium sulphate. After the solvent was removed, the residue was purified by silica column (eluent chloroform : methanol =

50 : 1) to get a light yellow solid in 65% yield. m.p. 57-59°C. IR (KBr): 3369.98, 2928.80, 1600.19, 1567.77, 1504.61, 1430.15, 1321.47, 1261.09, 1151.10, 1100.53, 978.93, 831.50, 772.07, 751.02, 696.22, 525.90, 472.22 cm^{-1} ; ^1H NMR (300 MHz, CDCl_3) δ (ppm) 8.09 (d, $J = 3.1$ Hz, 2H), 7.97 (d, $J = 6.7$ Hz, 2H), 7.75 (s, 1H), 7.54 (d, $J = 7.3$ Hz, 2H), 7.38 (d, $J = 7.5$ Hz, 3H), 7.29 (s, 4H), 7.03 (s, 2H), 6.50 (s, 2H), 6.42 (d, $J = 8.2$ Hz, 2H), 6.18 (s, 2H), 5.39 (s, 4H), 4.81 (s, 4H). ^{13}C NMR (100 MHz, CDCl_3): δ 158.38, 157.19, 154.03, 147.96, 139.64, 137.69, 137.20, 136.61, 128.91, 128.62, 126.48, 126.25, 120.41, 120.16, 112.85, 111.09, 108.22, 70.94, 47.72; MS: Calcd for: $[\text{M} + \text{H}]^+$: 605.27 ; Found: 605.34.

2.3. Spectrophotometric experiments

The probe **1** was dissolved in DMF solution. Before spectroscopic measurements, the solution was freshly prepared in hexamethylenetetramine–HCl (Tris) aqueous buffer (20 mmol L^{-1} , pH 7.4) by diluting the high concentration stock solution to 3.33×10^{-5} M (DMF: Tris=1:1, pH 7.4). Metal ions (0.1M, 10 mM tris buffer, pH 7.4) were detected by the addition of different volume stock solutions to probe **1** solution. The photophysical spectral changes of ligand with the metal ions such as Li^+ , Na^+ , K^+ , Ag^+ , Zn^{2+} , Mg^{2+} , Ba^{2+} , Ca^{2+} , Mn^{2+} , Pb^{2+} , Hg^{2+} , Ni^{2+} , Cd^{2+} , Co^{2+} , Cu^{2+} , Fe^{2+} , Cr^{3+} , Fe^{3+} and Al^{3+} were investigated by UV–vis and fluorescence spectra. The fluorescence emission spectra was recorded in the wavelength range from 300 to 700 nm with excitation wavelength at 295 nm. Both the excitation and emission slits were set at 5.0 nm.

2.4. Cell imaging

In vitro experiments were performed using HeLa cells. HeLa cells were cultured in Dulbecco modified Eagle medium, which were supplemented with 10% fetal bovine serum in an atmosphere of 5% CO_2 at 37 °C for 24 h. Before the experiments, the cells were incubated with 50 mM HL in 0.1M sterile PBS buffer for 30min at room temperature. After incubation, the cells were washed with PBS buffer and incubated with metal ions for additional 30 min under 5% CO_2 . The cells were washed three times with PBS buffer. Cells were seeded on dish for fluorescence microscopic imaging by inversion fluorescence microscope.

3. Results and discussion

3.1 pH effect of **1**

In order to eliminate the disturbance by H^+ during the detection of metal ions and to find optimal sensing conditions, the fluorescence intensity of compound **1** at various pH values in the presence and absence of metal ions were determined in DMF- H_2O (1:1, v/v). The effect of pH was evaluated in the pH range of 2–12 as shown in Fig. 1. It was clearly demonstrated that the probe **1**- Al^{3+} system shown strong fluorescence intensity at the pH less than 7.5 but decrease high than 7.5. This may be due to the protonation of N atom and the formation of $Al(OH)_3$, respectively. There were similar changes in the fluorescence intensity of the **1**+ Al^{3+} + Fe^{3+} system in different pH conditions. Therefore, it was demonstrated that probe **1** could be used under physiological conditions for biological applications with very low background fluorescence. All spectroscopic measurements were carried out under the physical conditions simulated the measurements of pH 7.4 at room temperature (10 mM tris buffer).

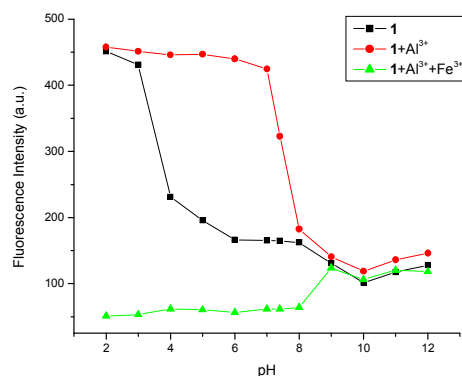


Fig. 1. Fluorescence intensity of probe **1** (DMF: Tris=1:1, pH=7.4, 3.33×10^{-5} M), $1+Al^{3+}$ (4.5 equiv.) and $1+Al^{3+}+Fe^{3+}$ (4.5 equiv.) at various pH values.

3.2 The selectivity of probe **1** to Al^{3+}

The fluorescence sensing ability of probe **1** was studied by addition of metal ions. The Fluorescence responses of probe **1** were shown in Fig. 2. The addition of Al^{3+} to a solution of **1** induced a significant enhancement of fluorescence intensity. However, under identical conditions, the fluorescence was completely quenched by addition of Fe^{3+} ions; nearly no fluorescence intensity changes were observed in emission spectra

with the other ions. The results indicated that probe **1** were a highly selective fluorescence “turn-on” probe for Al^{3+} and “turn-off” probe for Fe^{3+} . Achieving high selectivity toward Al^{3+} over the other competitive species coexisting was a very important feature to evaluate the performance of the fluorescent probe **1**. Therefore, the competition experiments were also conducted for probe **1**. Fig. 3 indicated that when Al^{3+} were added into the solution of probe **1** in the presence of other ions, the emission spectra displayed a similar pattern to that with Al^{3+} only except for Fe^{3+} ion. The competition experiments indicated that Fe^{3+} induced disturbance to Al^{3+} detection, which meant that probe **1** could perform as a highly selective probe for Al^{3+} via fluorescence “turn-on” mechanism. The competition experiments demonstrated eminent relay recognition of Fe^{3+} as well. So far, the “off-on-off” mechanism has been achieved with sequence specificity (Al^{3+} - Fe^{3+}).

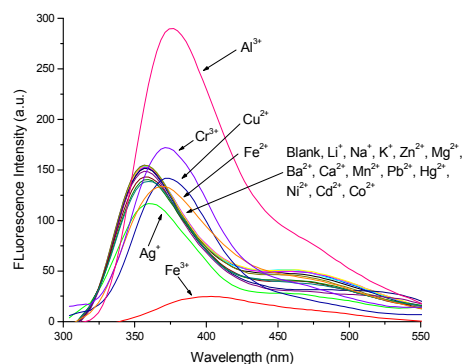


Fig. 2. Changes in fluorescent intensity ($\lambda_{\text{ex}}=295$ nm) of probe **1** upon the addition of different metal ions Li^+ , Na^+ , K^+ , Ag^+ , Zn^{2+} , Mg^{2+} , Ba^{2+} , Ca^{2+} , Mn^{2+} , Pb^{2+} , Hg^{2+} , Ni^{2+} , Cd^{2+} , Co^{2+} , Cu^{2+} , Fe^{2+} , Cr^{3+} , Fe^{3+} and Al^{3+} (4.5 equiv.).

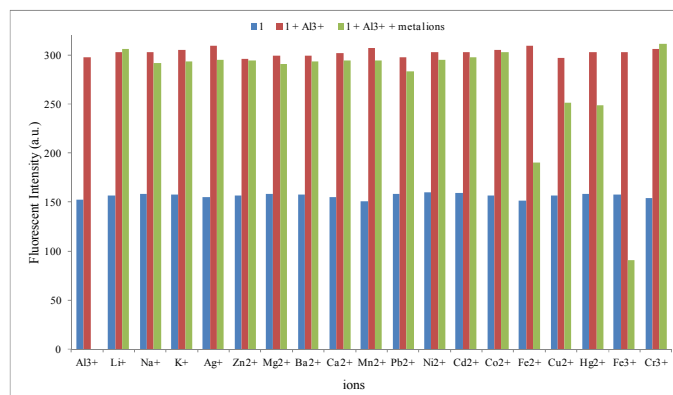


Fig. 3. The fluorescence intensity of solution probe **1** (DMF: Tris = 1:1, pH=7.4, 3.33×10^{-5} M) to various metal ions. The blue bars represent the fluorescence intensity of only probe **1**, the red bars represent the fluorescence intensity of the above solution upon subsequent addition of 4.5 equiv. of Al^{3+} . The green bars represent the fluorescence intensity of the above solution upon subsequent addition of 4.5 equivalent of Al^{3+} and 4.5 equiv. of other metal ions.

3.3. Absorption properties of probe **1**

The UV-vis absorption spectrum responses of probe **1** recognition of Al^{3+} and Fe^{3+} were also studied (Fig. 4). The absorption spectrum of free probe **1** exhibited only one absorbance peak at 300 nm. When 4.5 equiv. of Al^{3+} was added to the solution, the UV-vis response of probe **1** shown red shift of the maximum absorption, moreover, with the addition of 4.5 equiv. of Fe^{3+} to the $1+\text{Al}^{3+}$ system, the intensity of the absorption at about 302 nm increased. The UV-vis response of probe **1** shown red shift of the maximum absorption indicating the formation of a complex between probe **1** and metal ion. Furthermore, the band appearing in the UV-vis region (285–455 nm) which is typical for internal charge transfer (ICT) due to imines' linkage is characteristics of the ligand.

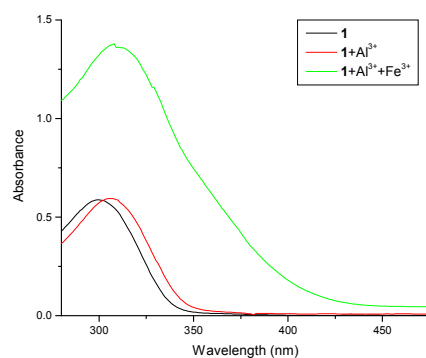


Fig. 4. UV-vis spectra of prob **1**(DMF: Tris = 1:1, pH = 7.4, 3.33×10^{-5} M), $1+\text{Al}^{3+}$ and $1+\text{Al}^{3+}+\text{Fe}^{3+}$.

3.4 Ions-titration and spectral responses

The fluorescence intensity changes of probe **1** in the presence of Al^{3+} were investigated. As shown in Fig. 5a, the free probe **1** (3.33×10^{-5} M) emitted fluorescence at 357 nm. The fluorescence intensity of probe **1** increased gradually with gradually red shifted to 375 nm on addition of Al^{3+} (0–4.5 equiv.), which agreed

with that in the UV–vis spectra. The obvious red shift could be explained that the ICT phenomenon was inhibited upon binding Al^{3+} ion. The coordination of Al^{3+} to probe **1** induces an intramolecular electron transfer process (ICT) from the nitrogen atom of the nitrogen atom of the quinoline was coordinated with Al^{3+} to cause an enhanced ICT process from donor (methoxy group) to acceptor (quinoline)^{35, 36}, so an obvious red shift in both fluorescence and absorption wavelength could be observed³⁷.

The binding association constant (K_a) the stoichiometry of **1**- Al^{3+} complex were determined from Benesi–Hildebrand equation by changes in the fluorogenic response in the presence of varying Al^{3+} concentrations between probe **1** and Al^{3+} . The results indicated the formation of a 1:1 complex and the binding association constant (K_a) was determined to be $2.11 \times 10^3 \text{ M}^{-1}$ (Fig. 5b). Moreover, the Job's plot analysis showed 1:1 binding stoichiometry complex between the probe **1** and Al^{3+} (Fig. 6)^{38, 39}. Additionally, the estimated limit of detection (LD) was came out to be $2.20 \times 10^{-6} \text{ M}$ for **1**- Al^{3+} complex (Fig. 7)⁴⁰. The results indicated that probe **1** was sensitive to Al^{3+} and could be potentially used to quantitatively detect Al^{3+} concentration.

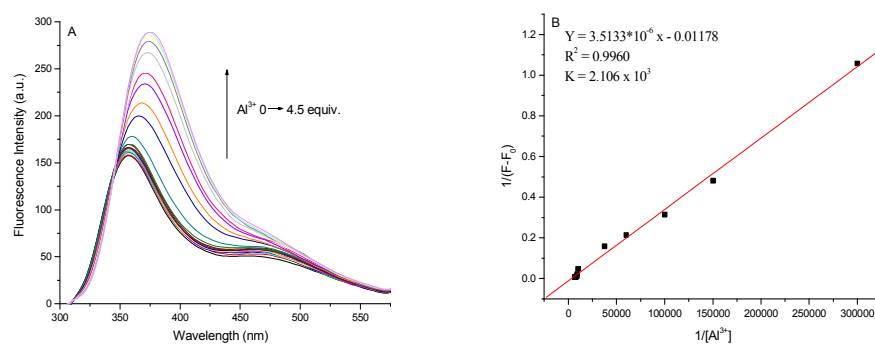


Fig.5(A). Fluorescent spectra of probe **1** (DMF: Tris = 1:1, pH = 7.4, $3.33 \times 10^{-5} \text{ M}$) with the addition of various concentration of Al^{3+} ($\lambda_{\text{ex}}=295 \text{ nm}$). (B). Benesi–Hildebrand plot of fluorescent probe (**1**+ Al^{3+}) at $\lambda_{\text{ex}} = 295 \text{ nm}$.

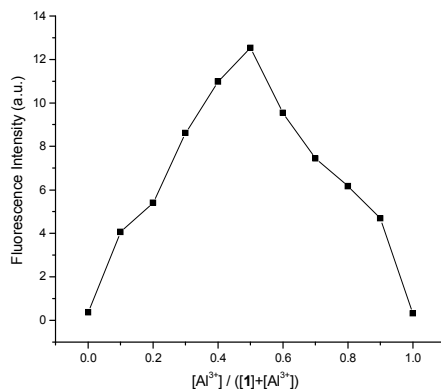


Fig. 6. 1:1 Stoichiometry of the host guest relationship was realized from the job's plot.

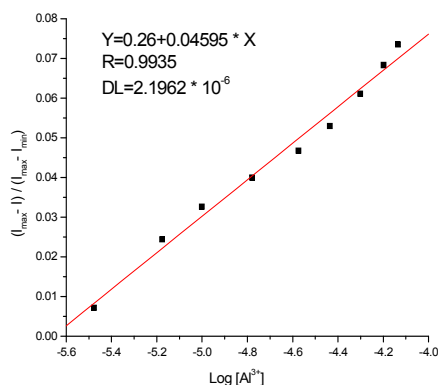


Fig. 7. The detection limit (DL) of probe **1** for Al³⁺ was calculated as 2.1962×10⁻⁶ M.

In the competition experiments, upon addition of Fe³⁺ to the 1-Al³⁺ system, as shown in Fig.8(a), with the addition of Fe³⁺ (0-13.0 equiv.) to the solution, the fluorescence intensity at 375 nm was dramatically decreased to quenching completely Fig.8(b) and gradually red shifted to 410 nm, the fluorescence was quenched and transformed into that of the L-Fe³⁺ system. Whereas upon addition of Al³⁺ to the 1-Fe³⁺ system, the fluorescence profile did not change obviously. Obviously, the fluorescence changes could be ascribed to the ligand-to-ligand charge transfer⁴¹, as illustrated in Fig. 9. When probe **1** coordinated with Fe³⁺ ions, the structure of **1**-Fe³⁺ became more stable than that of 1-Al³⁺. The selective fluorescence quenching of probe **1** upon Fe³⁺ ion addition may be due to paramagnetic nature of Fe³⁺ which on

coordination with the heteroatoms of ligands triggered the nonradiative deactivation process instead of fluorescent emission signal led to the efficient fluorescence quenching^{42, 43}. Besides, the above calculated binding constant of 1-Al³⁺-Fe³⁺ ($5.58 \times 10^3 \text{ M}^{-1}$) (Figs. 1). Thus, the Al³⁺ in the formed complex 1-Al³⁺ could be replaced by Fe³⁺ forming 1-Fe³⁺, accompanied by fluorescence quenching. The corresponding LOD was calculated to be $1.96 \times 10^{-5} \text{ M}$ (Figs. 2).

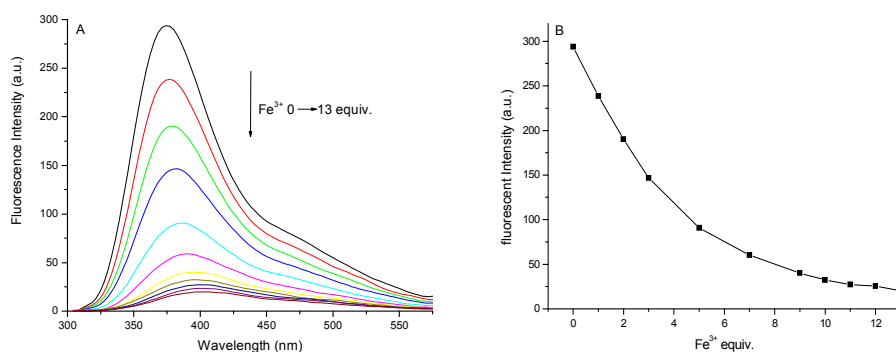


Fig. 8. A: Fluorescence emission spectra of 1+Al³⁺ upon addition of Fe³⁺ (0 to 13.0 equiv.) with an excitation of 295 nm. B: Changes of the emission intensity with the addition of Fe³⁺.

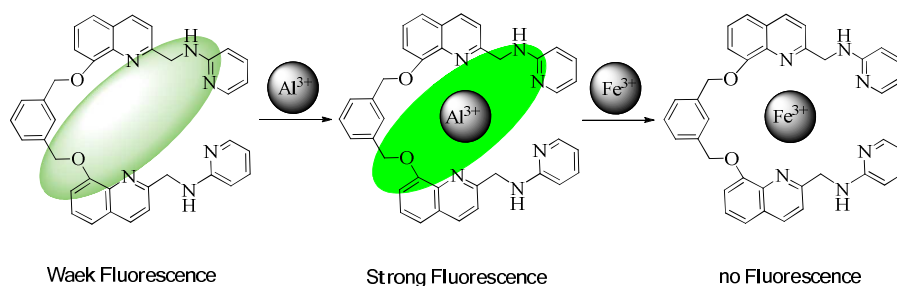


Fig. 9 The illustration of fluorescence “turn-on” of probe 1 for selective detection of Al³⁺ and fluorescence “turn-off” of probe 1 for selective detection of Fe³⁺.

3.5 Fluorescence imaging

To demonstrate the potential of probe 1 to image Al³⁺ and Fe³⁺ in living matrices, We next sought to investigate the utility of probe 1 for monitoring the intracellular (living Hela cells) exogenous Al³⁺ and Fe³⁺. As shown in Fig. 10, Hela cells treated with probe 1 (10 μM) alone in the growth medium for 30 min gave a very weak fluorescence (Fig.10 a–c), indicating the efficient loading of probe 1. When the cells

were further incubated with 20 μM Al^{3+} for 30 min, a bright blue fluorescence was observed (Fig.10 d–f). Bright field measurements after treatment with probe **1** and Al^{3+} confirmed that the cells were viable throughout the imaging experiments, showing the formation of the probe **1**- AlCl_3 complex in the cells. While for the cells incubated with probe **1** and FeCl_3 , the faint blue fluorescence disappeared and turned dark inside cells, attributed to the quenching role of FeCl_3 that got into the cells. Thus, probe **1** can detect intracellular Al^{3+} very efficiently.

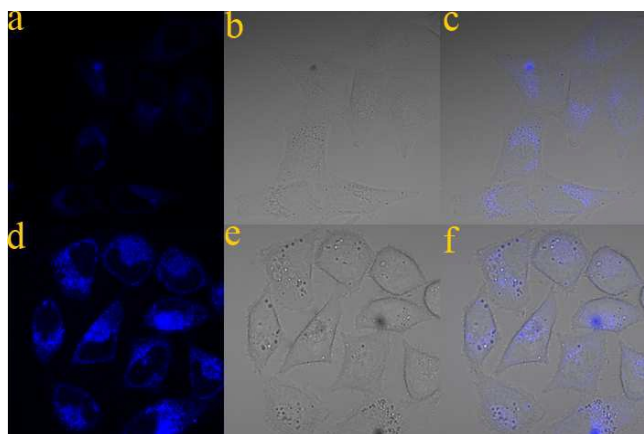


Fig. 10 Confocal fluorescence images of live HeLa cells. a) Bright-field transmission image of cells incubated with 10 μM probe **1** for 30 min; b) Bright image of the cells; c) Merged image of a and b; d) Fluorescence image when treated with sensor followed by 20 μM Al^{3+} ; e) Bright field image of d; f) An overlay image of d and e.

4. Conclusions

In summary, we synthesized a new quinoline-based fluorescent probe for Al^{3+} and Fe^{3+} . The probe displayed different fluorescence responses toward Al^{3+} (turn-on) and Fe^{3+} (turn-off) in aqueous environment, respectively, showing high sensitivity and selectivity. Probe exhibited a strong preference for Al^{3+} over other metal ions in DMF- H_2O solution. Importantly, probe- Al^{3+} shown high selectivity for Fe^{3+} over other metal ions, and could eliminate the interference of Al^{3+} during Fe^{3+} detection. These suggested that probe could serve as a nice probe for the detection of Al^{3+} and Fe^{3+} via the “off-on-off” mechanism with sequence specificity in DMF- H_2O solution. Finally, in living cell imaging demonstrated that the new probe was cell-permeable and could be used to monitor the Al^{3+} in biosystems. This work may provide a new strategy to design probes for discriminating Al^{3+} in biological systems.

Acknowledgements

We thank the Program for He'nan Innovative Research Team in University (15IRTSTHN005) and the National Natural Science Foundation of China (Grant No. U1404207) for financial support.

Supplementary data

Some plots of fluorescence spectrometry experiments, characterization of the compounds were given.

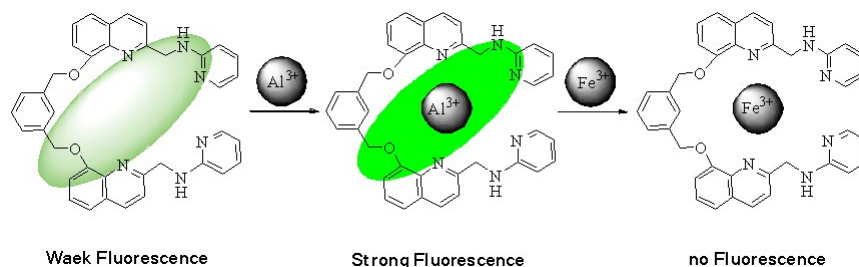
References

- 1 K.P. Carter, A.M. Young, A.E. Palmer, *Chem. Rev.*, 2014, **114**, 4564.
- 2 C. Xing, C. Hao, L. Liu, C. Xu, H. Kuang, *Food Agr. Immunol.*, 2014, **25**, 432.
- 3 C. Hao, L. Xua, C. Xing, H. Kuang, L. Wang, C. Xu, *Biosensors and Bioelectronics*, 2012, **36**, 174.
- 4 L. Xu, H. Yin, W. Ma, H. Kuang, L. Wang, C. Xu, *Biosensors and Bioelectronics*, 2015, **67**, 472.
- 5 C. Xing, L. Liu, S. Song, M. Feng, H. Kuang, C. Xu, *Biosensors and Bioelectronics*, 2015, **66**, 445.
- 6 X. Wu, L. Tang, W. Ma, L. Xu, L. Liu, H. Kuang, C. Xu, *RSC Adv.*, 2015, **5**, 81802.
- 7 G. Eskici, P.H. Axelsen, *Biochem.*, 2012, **51**, 6289.
- 8 M. Buchta, E. Kinesswetter, A. Otto, K.H. Schaller, A. Seeber, W. Hilla, K. Windorfer, J. Stork, A. Kuhlmann, O. Gefeller, S. Letzel, *Int. Arch. Occup. Environ. Health.*, 2003, **76**, 539.
- 9 Y.Z. Zhu, X.W. Li, C.X. Chen, F. Wang, J. Li, C.W. Hu, Y.F. Li, L.G. Miao, *Food. Chem. Toxicol.* 2012, **50**, 2911.
- 10 C.S. Cronan, W.J. Walker, P.R. Bloom, *Nature*, 1986, **324**, 140.
- 11 J.R. Walton, *J. Inorg. Biochem.*, 2007, **101**, 1275.
- 12 P. Nayak, *Environ. Res.*, 2002, **89**, 101.
- 13 G.D. Fasman, *Coord. Chem. Rev.*, 1996, **149**, 125.
- 14 J.H. Wang, D. Zhang, Y.Q. Liu, P.G. Ding, *Sens. Actuators B*, 2014, **191**, 344.
- 15 H.J. Sheng, X.M. Meng, W.P. Ye, Y. Feng, H.T. Sheng, X. Wang, Q.X. Guo, *Sens. Actuators B*, 2014, **195**, 534.
- 16 V.K. Gupta, A.K. Jain, S. Agarwal, G. Maheshwari, *Talanta*, 2007, **71**, 1964.
- 17 N.V. Ghule, R.S. Bhosale, A.L. Puyad, S.V. Bhosale, S.V. Bhosale, *Sensors and Actuators B*, 2016, **227**, 17.
- 18 V.K. Gupta, A.K. Singh, L.K. Kumawat, N. Mergu, *Sens. Actuators B*, 2016, **222**, 468.
- 19 F. Yan, T. Zheng, S. Guo, D. Shi, Z. Han, S. Zhou, L. Chen, *Spectrochim. Acta A* 2015, **151**, 881.
- 20 Y. Kang, X. Zheng, L. Jin, *J. Colloid Interface Sci.* 2016, **471**, 1.
- 21 S. Janakipriya, N.R. Chereddy, P. Korrapati, S. Thennarasu, A.B. Mandal, *Spectrochim. Acta A*, 2016, **153**, 465.
- 22 L. He, C. Liu, J.H. Xin, *Sensors and Actuators B*, 2015, **213**, 181.
- 23 P.N. Borase, P.B. Thale, S.K. Sahoo, G.S. *Sensors and Actuators B*, 2015, **215**,

- 451.
- 24 A. Singh, R. Singh, M. Shellaiah, E.C. Prakash, H.C. Chang, P. Raghunath, M.C. Linc, H.C. Lina, *Sensors and Actuators B*, 2015, **207**, 338.
- 25 X. Fang, S. Zhang, G. Zhao, W. Zhang, J. Xu, A. Ren, C. Wu, W. Yang, *Dyes Pigm.* 2014, **101**, 58.
- 26 G.M. Cockrell, G. Zhang, D.G. Van Derveer, R.P. Thummel, R.D. Hancock, *J. Am. Chem. Soc.*, 2008, **130**, 1420.
- 27 L. Praveen, V.B. Ganga, R. Tirumalai, T. Sreeja, M.L.P. Reddy, R.L. Varma, *Inorg. Chem.*, 2007, **46**, 6277.
- 28 N.A. El-Ghamaz, M.A. Diab, A.A. El-Bindary, A.Z. El-Sonbati, S.G. Nozha, *Spectrochim. Acta A*, 2015, **143**, 200.
- 29 M.R.E.S. Aly, H. Shokry, T. Sharshar, M.A. Amin, *J. Mol. Liq.*, 2016, **214**, 319.
- 30 L. Aboutorabi, A. Morsali, *Coord. Chem. Rev.*, 2016, **310**, 116.
- 31 S. Hu, J. Song, G. Wu, C. Cheng, Q. Gao, *Spectrochim. Acta A*, 2015, **136**, 1188.
- 32 Launay, V. Alain, E. Destandau, N. Ramos, E. Bardez, P. Baret, J.L. Pierre, *New J. Chem.*, 2001, **25**, 1269.
- 33 W. Xu, Y. Zhou, D. Huang, M. Su, K. Wang, M. Hong, *Inorg. Chem.* 2014, **53**, 6497.
- 34 R. Patil, A. Moirangthem, R. Butcher, N. Singh, A. Basu, K. Tayade, U. Fegade, D. Hundiware, A. Kuwar, *Dalton Trans.*, 2014, **43**, 2895.
- 35 C.L. Lu, Z.C. Xu, J.N. Cui, R. Zhang, X.H. Qian, *J. Org. Chem.*, 2007, **72**, 3554.
- 36 X.M. Meng, S.X. Wang, Y.M. Li, M.Z. Zhu, Q.X. Guo, *Chem. Commun.*, 2012, **48**, 4196.
- 37 Z. Shi, Q. Han, L. Yang, H. Yang, X. Tang, W. Dou, Z. Li, Y. Zhang, Y. Shao, L. Guan, W. Liu, *Chem. Eur. J.*, 2015, **21**, 290.
- 38 P. Song, C. Wang, P. Wang, X. Liu, K. Xu, *Chin. J. Org. Chem.*, 2016, **36**, 782.
- 39 K.X. Xu, H.J. Kong, Q. Li, P. Song, Y.P. Dai, L. Yang, *Spectrochim. Acta A*, 2015, **137**, 957.
- 40 Y. Dai, K. Xu, Q. Li, C. Wang, X. Liu, P. Wang, *Spectrochim. Acta A*, 2016, **157**, 1.
- 41 H.L. Lu, W.K. Wang, X.X. Tan, X.F. Luo, M.L. Zhang, M. Zhang, S.Q. Zang, *Dalton Trans.*, 2016, **45**, 8174.
- 42 J. Mao, L. Wang, W. Dou, X.L. Tang, Y. Yan, W.S. Liu, *Org. Lett.*, 2007, **9**, 4567.
- 43 M. Saleem, S.K. Kang, K. H. Lee, *J. Lumin.*, 2015, **162**, 14.

A new fluorescent probe based on quinoline for detection of Al^{3+} and Fe^{3+} with “off-on-off” response in aqueous solution

Yanpeng Dai^a, Kuoxi Xu^{a, b*}, Xiaoyan Liu^a, Peng Wang^a, Jiaxin Fu^a, Kun Yao^a



A new quinoline-based fluorescent probe for Al^{3+} and Fe^{3+} has been designed and synthesized. It showed highly selective relay recognition of Al^{3+} and Fe^{3+} via a fluorescence “off-on-off” mechanism by central metal displacement. The living HeLa cells imaging studies revealed that the probe was cell-permeable and could be used to detect intracellular Al^{3+} and Fe^{3+} ion.